Supplementary Online Material

Wavelet Measurement Suggests Cause of Period Instability in Mammalian Circadian Neurons

Kirsten Meeker[1], Richard Harang[2], Alexis B. Webb[3], David K. Welsh[4], Francis J. Doyle III[5], Guillaume Bonnet[2], Erik D. Herzog[3], Linda R. Petzold[1]

[1]Department of Computer Science, University of California, Santa Barbara, CA

[2]Department of Statistics and Applied Probability, University of California, Santa Barbara, CA

[3]Department of Biology, Washington University, St. Louis, MO

[4]Department of Psychiatry, University of California, San Diego, La Jolla, CA

Center for Chronobiology, University of California, San Diego, La Jolla, CA

Veterans Affairs San Diego Healthcare System, San Diego, CA

[5]Department of Chemical Engineering, University of California, Santa Barbara, CA

Discrete Stochastic Circadian Model

This model is the discrete stochastic version constructed from Leloup and Goldbeter's (Leloup and Goldbeter, 2003) 16-state mammalian model. In Tables S1 and S2, we list the reactions involved in a single cell. To convert molar concentrations in the deterministic model to populations (number of each chemical species) requires converting the concentration to units of molecules per liter then multiplying by a cell volume V. The scaling constant Ω is given by

$$\Omega = N_A \text{ [molecules/liter]} \times V \text{ [liters]}, \tag{1}$$

where Avogadro's number $N_A = 6.022 \times 10^{23}$.

Statistical analysis of long periods

Statistical analysis of the significance of the long periods was carried out using three separate models for noise. To evaluate the possibility that Poisson-distributed noise arising from the stochastic nature of photon emissions was responsible for the appearance of long periods, testing was carried out against the null hypothesis of a homogenous Poisson process. To evaluate the possibility that the combination of a serially correlated process and CWT analysis was generating spurious long-period signals, a population-based analysis was carried out using a null hypothesis of $1/f$-type noise; a stochastic process with significant serial correlations. Finally, an analysis was carried out using bioluminesence data from BMAL1 knockout cells as a null distribution; deletion of BMAL1 is known to remove circadian behavior in whole animals, thus use of this data as a null distribution allows us to compare known aperiodic data against the test data to determine statistical significance.

As the CWT analysis bins periodic behavior into a discrete but user-selectable number of levels, the distributions of periods in traces from individual cells were treated as observations drawn from a single multinomial distribution with unknown parameter vector $\hat{p}_i$, with different values of $i \in \{1, 2, 3, 4\}$ denoting the 4 possible combinations of data sets (Webb et al. versus Liu et al.) and cell type (SCN slice data versus SCN dispersed data). Under the assumption that $\hat{p}_i$ has a prior distribution of a Dirichlet distribution with a diffuse, noninformative prior parameter $\alpha_{\text{prior}} = [0.1\,, 0.1\,, \ldots 0.1]$, we may use straightforward conjugate analysis (see, e.g. Robert and Casella (2004)) to determine the posterior density of $\hat{p}_i$. Having observed a series of observations X, we may readily find that $\hat{p}_i \mid X$ is likewise Dirichlet-distributed with a posterior parameter $\alpha_{\text{posterior}} = \alpha_{\text{prior}} + \sum_{i=1}^{n} X^{(i)}$. Random draws from the posterior distribution were generated by sampling and renormalizing Gamma random variables using the "gamrnd" function of the MATLAB statistics toolbox.

To determine statistical significance against $1/f$-type noise and BMAL1

knockout data, posterior distributions for each were generated from the CWT of the processes as described above. A sampled value of either $\hat{p}_{1/f}$ or $\hat{p}_{\mathrm{KO}}$ was then drawn, and compared to a sample drawn from the distribution $\hat{p}_i$ under consideration. The values of $\hat{p}_i$ above the values of either $\hat{p}_{1/f}$ or $\hat{p}_{\mathrm{KO}}$, as appropriate, were determined. This pairwise comparison process was repeated 100,000 times, allowing us to estimate the probability that a random observation from our null distribution would be greater than a random observation from our test distribution along a variety of infradian periods, thus calculating a series of p-values. Testing of SCN slice data via this method produced absolutely no statistically significant infradian periods of length greater than 36 hours, and plots are thus omitted. Testing of SCN dispersed data infradian periodicities revealed some periodicities that were statistically significant at the $p < 0.01$ level against null hypotheses of both $1/f$-type noise and BMAL1 knockout data for dispersed cells from both Webb et al. (2009) and Liu et al. (2007) (Figure S7).

Significantly, the BMAL1 knockout data appears to have slightly elevated power in the period range of roughly 40 to 46 hours (see Figure S8); this led to no statistically significant periods in this range for the Webb et al. data evaluated against the BMAL1 knockout distribution, and very few statistically significant periods for the Liu et al. data. It should be noted that the stochastic model best able to reproduce the period distribution of dispersed cells involves increasing the Bmal1 repression rate, thus lowering the protein count of this species. This further supports the hypothesis that low levels of BMAL1 protein in the SCN contribute towards a tendency to longer periods and suggests that the BMAL1 knockout data may not be perfectly appropriate for modeling complete arrhythmicity in individual cells.

To determine statistical significance against a homogenous Poisson process, a different approach was needed due to the manner in which the spectral characteristics (and hence corresponding CWT) of a Poisson process change with the mean of the process. Rather than constructing a population density estimate,

we instead constructed cell by cell density estimates for dispersed cells from both Webb et al. and Liu et al., and compared them to an upper 99% quantile of the corresponding Poisson noise process of equal mean (see Figure S6, D,E,F for an example). As above, statistical significance was evaluated across all periods. We then tabulated the proportion of cells that contained statistically significant power at the $p < 0.01$ level against the null hypothesis of Poisson noise (the proportion of cells in which the blue line exceeded the green line at the indicated period). The resulting plots are displayed in Figure S5. In both cases, a significant number of cells are observed to have some long-period oscillations with high statistical significance.

We conclude that the long-period observations cannot be solely attributed to either a) an unforeseen interaction of the CWT with a serially correlated process, or b) the effect of shot noise on the individual cell observations. While analysis against a null distribution of BMAL1 knockout data greatly reduces the appearance of statistically significant periods in the 40 to 46 hours range, this is consistent with our modeling hypothesis that reduced expression of BMAL1 plays a key role in the appearance of these longer periods in dispersed cells.

Wavelet analysis of synthetic data sets

The effect of a single skipped period and the advantage of the CWT over standard Fourier methods for analyzing nonstationary data are highlighted below. A single skipped period due to either interfering noise or lack of data does not significantly affect the estimate of instantaneous period using the CWT (Figure S9). This property highlights the robustness of the CWT in evaluating instantaneous periods.

The advantage of the CWT over the Fourier transform for analysis of period in nonstationary oscillators is illustrated in Figure S10; the use of the Fourier transform incorrectly identifies a single period at roughly the average period for the entire signal, while the CWT accurately identifies the nonstationary nature of the oscillator, and provides good estimates for the changing period of the oscillator over time.

References

Jean-Christophe Leloup and Albert Goldbeter. Toward a detailed computational model for the mammalian circadian clock. *PNAS*, 100(12):7051–7056, 2003.

Andrew C. Liu, David K. Welsh, Caroline H. Ko, Hien G. Tran, Eric E. Zhang, Aaron A. Priest, Ethan D. Buhr, Oded Singer, Kirsten Meeker, Inder M. Verma, Francis J. Doyle III, Joseph S. Takahashi, and Steve A. Kay. Intercellular coupling confers robustness against mutations in the scn circadian clock network. *Cell*, 129(3):605–616, May 2007. URL `http://www.sciencedirect.com/science/article/B6WSN-4NMMB5G-R/2/4b4958b5013f5671cbd68a0246cfd69d`.

Christian P. Robert and George Casella. *Monte Carlo statistical methods*. Springer, 2004. ISBN 9780387212395.

Alexis B. Webb, Nikhil Angelo, James E. Huettner, and Erik D. Herzog. Intrinsic, nondeterministic circadian rhythm generation in identified mammalian neurons. *Proceedings of the National Academy of Sciences*, 106(38):16493–16498, 2009. doi: 10.1073/pnas.0902768106. URL `http://www.pnas.org/content/106/38/16493.abstract`.

Table S1: Reactions 1 – 27 in discrete stochastic model based on 16 state Leloup & Goldbeter model

	Reaction	Probability of reaction	Transitions
0	$G \rightarrow G + M_P$	$w_0 = (\nu_{sP}\Omega)\frac{B_N^n}{(K_{AP}\Omega)^n + B_N^n}$	$M_P \rightarrow M_P + 1$
1	$M_P \rightarrow$	$w_1 = (\nu_{mP}\Omega)\frac{M_P}{(K_{mP}\Omega) + M_P}$	$M_P \rightarrow M_P - 1$
2	$M_P \rightarrow$	$w_2 = k_{dmp} M_P$	$M_P \rightarrow M_P - 1$
3	$G \rightarrow G + M_C$	$w_3 = (\nu_{sC}\Omega)\frac{B_N^n}{(K_{AC}\Omega)^n + B_N^n}$	$M_C \rightarrow M_C + 1$
4	$M_C \rightarrow$	$w_4 = (\nu_{mC}\Omega)\frac{M_C}{(K_{mC}\Omega) + M_C}$	$M_C \rightarrow M_C - 1$
5	$M_C \rightarrow$	$w_5 = k_{dmc} M_C$	$M_C \rightarrow M_C - 1$
6	$G \rightarrow G + M_B$	$w_6 = (\nu_{sB}\Omega)\frac{(K_{IB}\Omega)^m}{(K_{IB}\Omega)^m + B_N^m}$	$M_B \rightarrow M_B + 1$
7	$M_B \rightarrow$	$w_7 = (\nu_{mb}\Omega)\frac{M_B}{(K_{mB}\Omega) + M_B}$	$M_B \rightarrow M_B - 1$
8	$M_B \rightarrow$	$w_8 = k_{dmb} M_B$	$M_B \rightarrow M_B - 1$
9	$M_P \rightarrow P_C$	$w_9 = k_{sp} M_P$	$P_C \rightarrow P_C + 1$
10	$P_C \rightarrow P_{CP}$	$w_{10} = (V_{1P}\Omega)\frac{P_C}{(K_p\Omega) + P_C}$	$P_C \rightarrow P_C - 1, P_{CP} \rightarrow P_{CP} + 1$
11	$P_{CP} \rightarrow P_C$	$w_{11} = (V_{2P}\Omega)\frac{P_{CP}}{(K_{dp}\Omega) + P_{CP}}$	$P_C \rightarrow P_C + 1, P_{CP} \rightarrow P_{CP} - 1$
12	$PC_C \rightarrow P_C + C_C$	$w_{12} = k_4 PC_C$	$P_C \rightarrow P_C + 1, C_C \rightarrow C_C + 1$ $PC_C \rightarrow PC_C - 1$
13	$P_C + C_C \rightarrow PC_C$	$w_{13} = (\frac{k_3}{\Omega})P_C C_C$	$P_C \rightarrow P_C - 1, C_C \rightarrow C_C - 1$ $PC_C \rightarrow PC_C + 1$
14	$P_C \rightarrow$	$w_{14} = k_{dn} P_C$	$P_C \rightarrow P_C - 1$
15	$M_C \rightarrow C_C$	$w_{15} = k_{sC} M_C$	$C_C \rightarrow C_C + 1$
16	$C_C \rightarrow C_{CP}$	$w_{16} = (V_{1C}\Omega)\frac{C_C}{(K_p\Omega) + C_C}$	$C_C \rightarrow C_C - 1, C_{CP} \rightarrow C_{CP} + 1$
17	$C_{CP} \rightarrow C_C$	$w_{17} = (V_{2C}\Omega)\frac{C_{CP}}{(K_{dp}\Omega) + C_{CP}}$	$C_C \rightarrow C_C + 1, C_{CP} \rightarrow C_{CP} - 1$
18	$C_C \rightarrow$	$w_{18} = k_{dnc} C_C$	$C_C \rightarrow C_C - 1$
19	$P_{CP} \rightarrow$	$w_{19} = (\nu_{dPC}\Omega)\frac{P_{CP}}{(K_d\Omega) + P_{CP}}$	$P_{CP} \rightarrow P_{CP} - 1$
20	$P_{CP} \rightarrow$	$w_{20} = k_{dn} P_{CP}$	$P_{CP} \rightarrow P_{CP} - 1$
21	$C_{CP} \rightarrow$	$w_{21} = (\nu_{dCC}\Omega)\frac{C_{CP}}{(K_d\Omega) + C_{CP}}$	$C_{CP} \rightarrow C_{CP} - 1$
22	$C_{CP} \rightarrow$	$w_{22} = k_{dn} C_{CP}$	$C_{CP} \rightarrow C_{CP} - 1$
23	$PC_C \rightarrow PC_{CP}$	$w_{23} = (V_{1PC}\Omega)\frac{PC_C}{(K_p\Omega) + PC_C}$	$PC_C \rightarrow PC_C - 1, PC_{CP} \rightarrow PC_{CP} + 1$
24	$PC_{CP} \rightarrow PC_C$	$w_{24} = (V_{2PC}\Omega)\frac{PC_{CP}}{(K_{dp}\Omega) + PC_{CP}}$	$PC_C \rightarrow PC_C + 1, PC_{CP} \rightarrow PC_{CP} - 1$
25	$PC_N \rightarrow PC_C$	$w_{25} = k_2 PC_N$	$PC_C \rightarrow PC_C + 1, PC_N \rightarrow PC_N - 1$
26	$PC_C \rightarrow PC_N$	$w_{26} = k_1 PC_C$	$PC_C \rightarrow PC_C - 1, PC_N \rightarrow PC_N + 1$
27	$PC_C \rightarrow$	$w_{27} = k_{dn} PC_C$	$PC_C \rightarrow PC_C - 1$

Table S2: Reactions 28 – 51 in discrete stochastic model based on 16 state Leloup & Goldbeter model

	Reaction	Probability of reaction	Transition
28	$PC_N \rightarrow PC_{NP}$	$w_{28} = (V_{3PC}\Omega)\frac{PC_N}{(K_p\Omega)+PC_N}$	$PC_N \rightarrow PC_N - 1, PC_{NP} \rightarrow PC_{NP} + 1$
29	$PC_{NP} \rightarrow PC_N$	$w_{29} = (V_{4PC}\Omega)\frac{PC_{NP}}{(K_{dp}\Omega)+PC_{NP}}$	$PC_N \rightarrow PC_N + 1, PC_{NP} \rightarrow PC_{NP} - 1$
30	$PC_N + B_N \rightarrow I_N$	$w_{30} = (\frac{k_7}{\Omega})PC_N B_N$	$PC_N \rightarrow PC_N - 1, B_N \rightarrow B_N - 1$ $I_N \rightarrow I_N + 1$
31	$I_N \rightarrow PC_N + B_N$	$w_{31} = k_8 I_N$	$PC_N \rightarrow PC_N + 1, B_N \rightarrow B_N + 1$ $I_N \rightarrow I_N - 1$
32	$PC_N \rightarrow$	$w_{32} = k_{dn} PC_N$	$PC_N \rightarrow PC_N - 1$
33	$PC_{CP} \rightarrow$	$w_{33} = (V_{dPCC}\Omega)\frac{PC_{CP}}{(K_d\Omega)+PC_{CP}}$	$PC_{CP} \rightarrow PC_{CP} - 1$
34	$PC_{CP} \rightarrow$	$w_{34} = k_{dn} PC_{CP}$	$PC_{CP} \rightarrow PC_{CP} - 1$
35	$PC_{NP} \rightarrow$	$w_{35} = (V_{dPCN}\Omega)\frac{PC_{NP}}{(K_d\Omega)+PC_{NP}}$	$PC_{NP} \rightarrow PC_{NP} - 1$
36	$PC_{NP} \rightarrow$	$w_{36} = k_{dn} PC_{NP}$	$PC_{NP} \rightarrow PC_{NP} - 1$
37	$M_B \rightarrow B_C$	$w_{37} = k_{sB} M_B$	$B_C \rightarrow B_C + 1$
38	$B_C \rightarrow B_{CP}$	$w_{38} = (V_{1B}\Omega)\frac{B_C}{(K_p\Omega)+B_C}$	$B_C \rightarrow B_C - 1, B_{CP} \rightarrow B_{CP} + 1$
39	$B_{CP} \rightarrow B_C$	$w_{39} = (V_{2B}\Omega)\frac{B_{CP}}{(K_{dp}\Omega)+B_{CP}}$	$B_C \rightarrow B_C + 1, B_{CP} \rightarrow B_{CP} - 1$
40	$B_C \rightarrow B_N$	$w_{40} = k_5 B_C$	$B_C \rightarrow B_C - 1, B_N \rightarrow B_N + 1$
41	$B_N \rightarrow B_C$	$w_{41} = k_6 B_N$	$B_C \rightarrow B_C + 1, B_N \rightarrow B_N - 1$
42	$B_C \rightarrow$	$w_{42} = k_{dn} B_C$	$B_C \rightarrow B_C - 1$
43	$B_{CP} \rightarrow$	$w_{43} = (V_{dBC}\Omega)\frac{B_{CP}}{(K_d\Omega)+B_{CP}}$	$B_{CP} \rightarrow B_{CP} - 1$
44	$B_{CP} \rightarrow$	$w_{44} = k_{dn} B_{CP}$	$B_{CP} \rightarrow B_{CP} - 1$
45	$B_N \rightarrow B_{NP}$	$w_{45} = (V_{3B}\Omega)\frac{B_N}{(K_p\Omega)+B_N}$	$B_N \rightarrow B_N - 1, B_{NP} \rightarrow B_{NP} + 1$
46	$B_{NP} \rightarrow B_N$	$w_{46} = (V_{4B}\Omega)\frac{B_{NP}}{(K_{dp}\Omega)+B_{NP}}$	$B_N \rightarrow B_N + 1\, B_{NP} \rightarrow B_{NP} - 1$
47	$B_N \rightarrow$	$w_{47} = k_{dn} B_N$	$B_N \rightarrow B_N - 1$
48	$B_{NP} \rightarrow$	$w_{48} = (V_{dBN}\Omega)\frac{B_{NP}}{(K_d\Omega)+B_{NP}}$	$B_{NP} \rightarrow B_{NP} - 1$
49	$B_{NP} \rightarrow$	$w_{49} = k_{dn} B_{NP}$	$B_{NP} \rightarrow B_{NP} - 1$
50	$I_N \rightarrow$	$w_{50} = (V_{dIN}\Omega)\frac{I_N}{(K_d\Omega)+I_N}$	$I_N \rightarrow I_N - 1$
51	$I_N \rightarrow$	$w_{51} = k_{dn} I_N$	$I_N \rightarrow I_N - 1$

Table S3: Default model parameter values

Parameter	Value	Parameter	Value
$k_1(h^{-1})$	0.4	$V_{1B}(nM^{-1} \cdot h^{-1})$	0.5
$k_2(h^{-1})$	0.2	$V_{1C}(nM^{-1} \cdot h^{-1})$	0.6
$k_3(nM^{-1} \cdot h^{-1})$	0.4	$V_{1P}(nM^{-1} \cdot h^{-1})$	0.4
$k_4(h^{-1})$	0.2	$V_{1PC}(nM^{-1} \cdot h^{-1})$	0.4
$k_5(h^{-1})$	0.4	$V_{2B}(nM^{-1} \cdot h^{-1})$	0.1
$k_6(h^{-1})$	0.4	$V_{2C}(nM^{-1} \cdot h^{-1})$	0.1
$k_7(nM^{-1} \cdot h^{-1})$	0.5	$V_{2P}(nM^{-1} \cdot h^{-1})$	0.3
$k_8(h^{-1})$	0.1	$V_{2PC}(nM^{-1} \cdot h^{-1})$	0.1
$k_{AP}(nM)$	0.7	$V_{3B}(nM^{-1} \cdot h^{-1})$	0.5
$k_{AC}(nM)$	0.6	$V_{3PC}(nM^{-1} \cdot h^{-1})$	0.4
$k_{IB}(nM)$	2.2	$V_{4B}(nM^{-1} \cdot h^{-1})$	0.2
$k_{dmb}(h^{-1})$	0.01	$V_{4PC}(nM^{-1} \cdot h^{-1})$	0.1
$k_{dmc}(h^{-1})$	0.01	$V_{phos}(nM^{-1} \cdot h^{-1})$	0.4
$k_{dmp}(h^{-1})$	0.01	$\nu_{dBC}(nM^{-1} \cdot h^{-1})$	0.5
$k_{dn}(h^{-1})$	0.01	$\nu_{dBN}(nM^{-1} \cdot h^{-1})$	0.6
$k_{dnc}(h^{-1})$	0.12	$\nu_{dCC}(nM^{-1} \cdot h^{-1})$	0.7
$K_d(nM)$	0.3	$\nu_{dIN}(nM^{-1} \cdot h^{-1})$	0.8
$K_{dp}(nM)$	0.1	$\nu_{dPC}(nM^{-1} \cdot h^{-1})$	0.7
$K_p(nM)$	0.1	$\nu_{dPCC}(nM^{-1} \cdot h^{-1})$	0.7
$K_{mB}(nM)$	0.4	$\nu_{dPCN}(nM^{-1} \cdot h^{-1})$	0.7
$K_{mC}(nM)$	0.4	$\nu_{mB}(nM^{-1} \cdot h^{-1})$	0.8
$K_{mP}(nM)$	0.31	$\nu_{mC}(nM^{-1} \cdot h^{-1})$	1.0
$k_{sB}(h^{-1})$	0.12	$\nu_{mP}(nM^{-1} \cdot h^{-1})$	1.1
$k_{sC}(h^{-1})$	1.6	$\nu_{sB}(nM^{-1} \cdot h^{-1})$	1.0
$k_{sP}(h^{-1})$	0.6	$\nu_{sC}(nM^{-1} \cdot h^{-1})$	1.1
m	2	$\nu_{sP}(nM^{-1} \cdot h^{-1})$	1.5
n	4	Ω	25

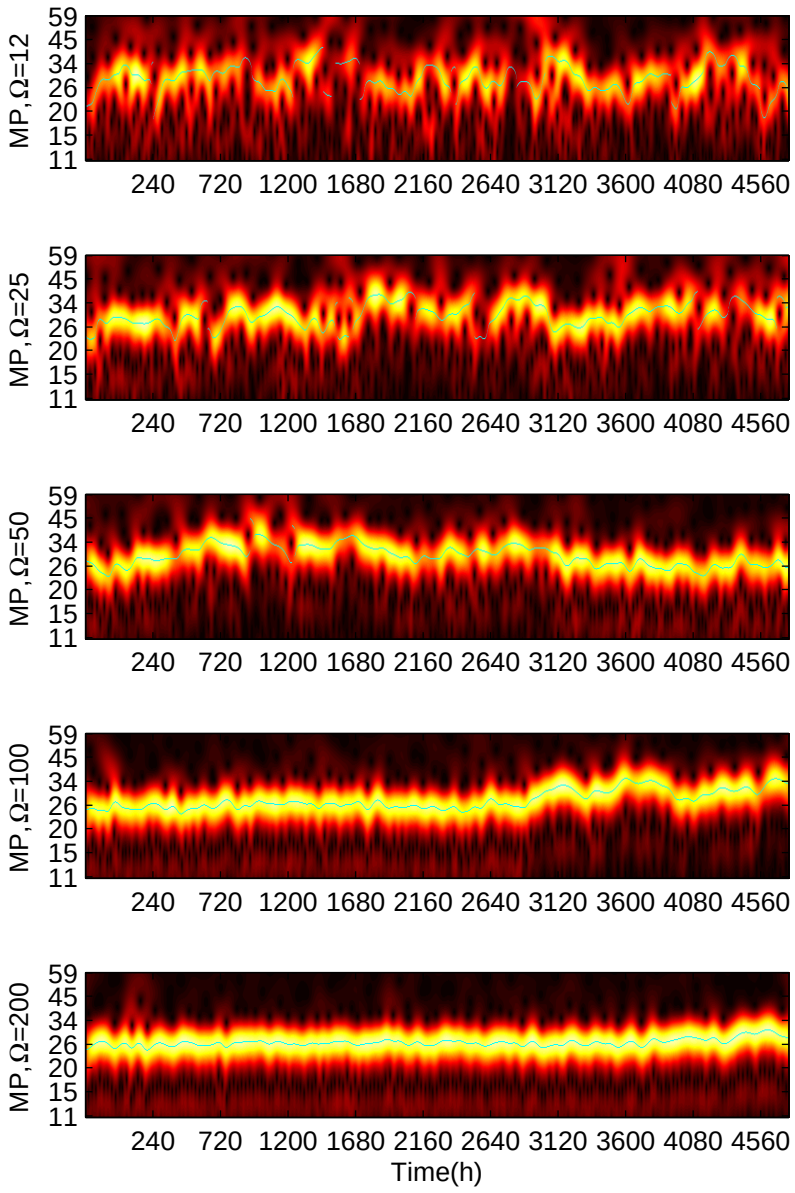

Figure S1: Period variability is reduced in the stochastic $K_{IB} = 4$ model as the number of molecules is increased (with increasing Ω top to bottom).

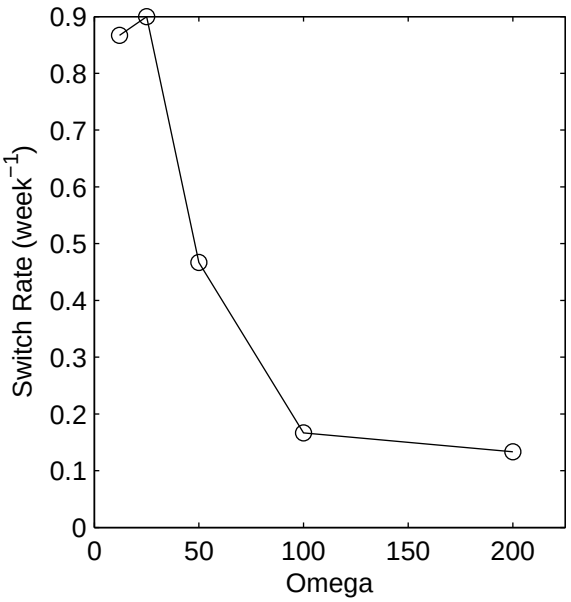

Figure S2: Switching rate from circadian to infradian periods (30 h. crossings) as a function of Ω. In the deterministic limit (at large Ω) the switching rate goes to zero.

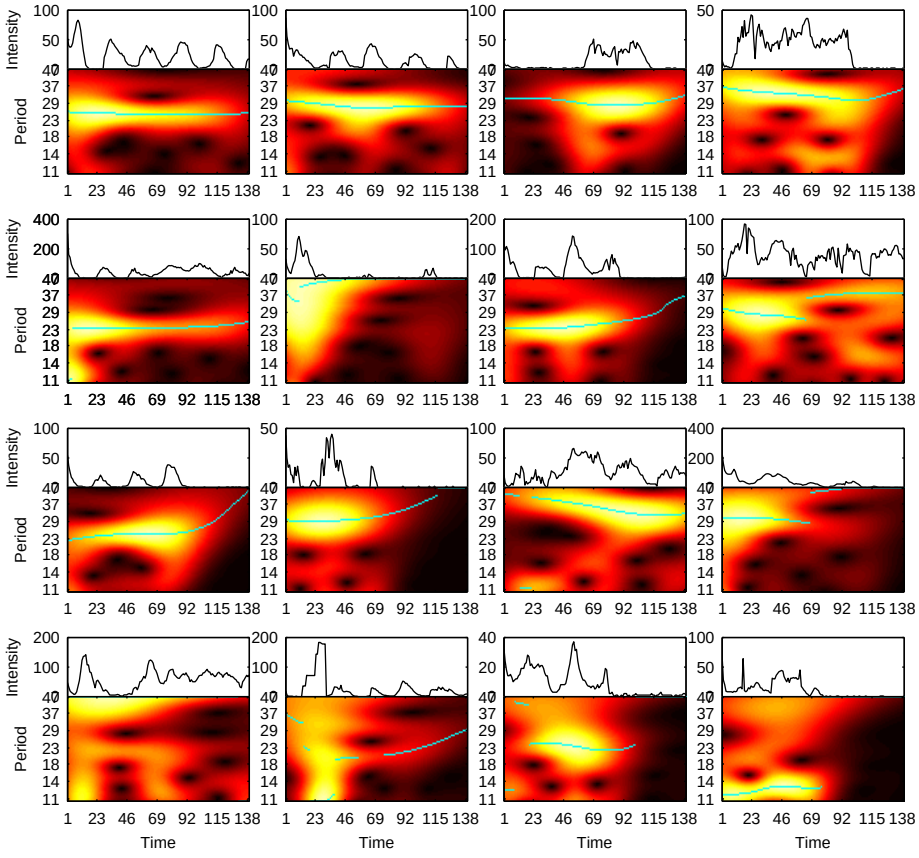

Figure S3: Visualization of the range of circadian behaviors possible in dispersed SCN cells. Cells are displayed in order of increasing period variance, from left to right and top to bottom. Sixteen uniformly spaced cells across the length of the data set were selected, transformed, and plotted. Sampled from n=322 cells from Webb et al. (2009).

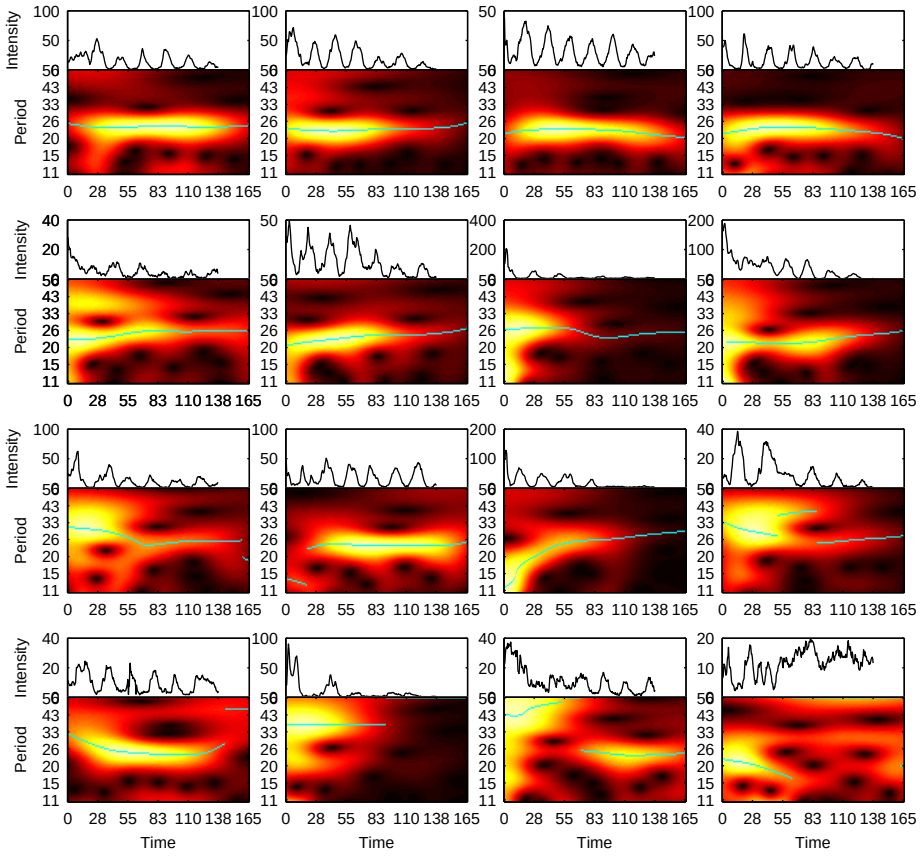

Figure S4: Visualization of the range of circadian behaviors possible in dispersed SCN cells, as in figure S3, above. Sampled from n=310 dispersed cells from Liu et al. (2007).

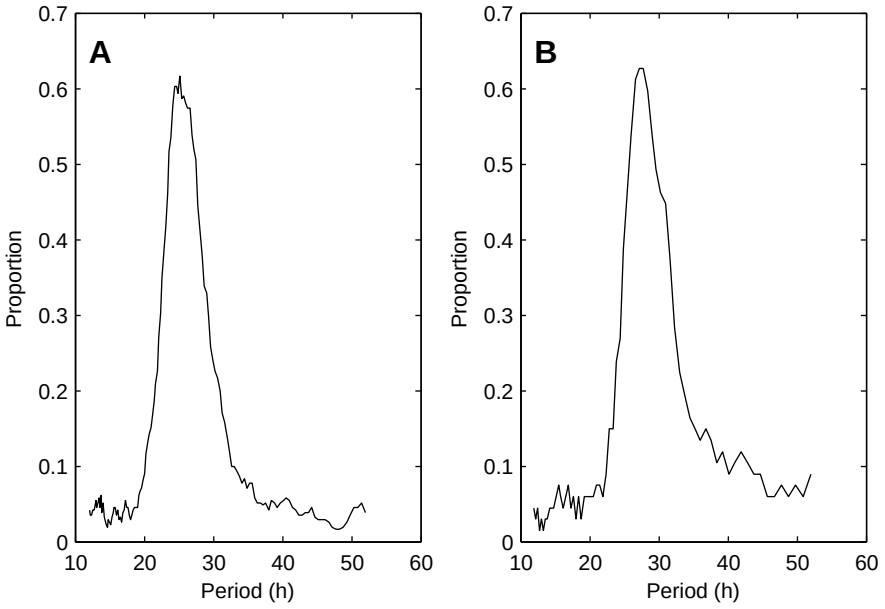

Figure S5: Graphical summary of statistical testing against the null hypotheses of a homogeneous Poisson process. Panel A shows the results from 322 dispersed cells from the Webb et al. (2009). The vertical axis indicates the percentage of all cells observed that displayed statistically significant periodicities (p-value of < 0.01) as determined by the CWT ridge for the period indicated on the horizontal axis. Note that most dispersed SCN cells express measurable periods in the circadian range over the length of the recording. Panel B shows the results from statistical testing of 310 dispersed cells from Liu et al. (2007) against null hypotheses of a homogenous Poisson process. Axes and p-value as in panel A.

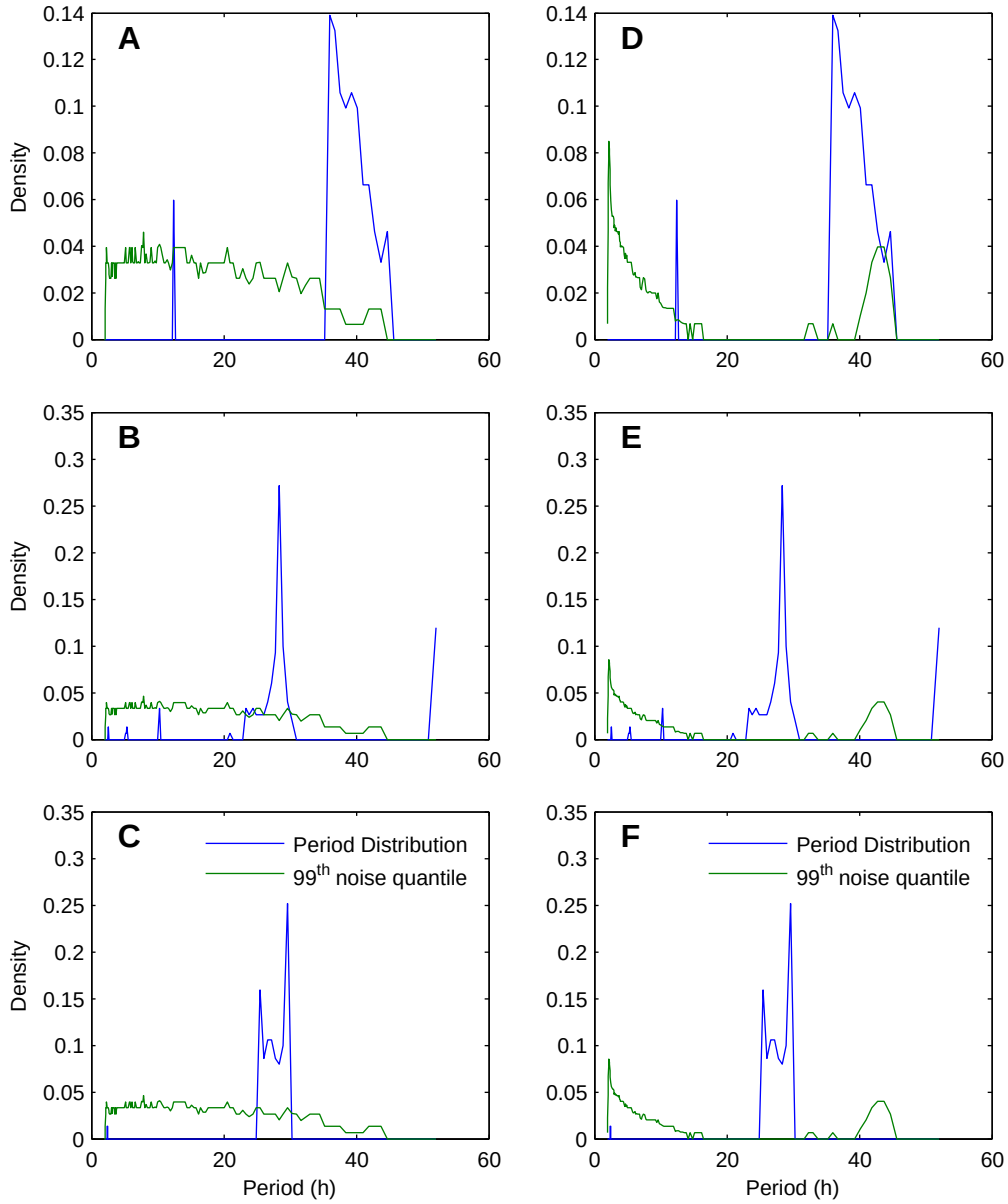

Figure S6: Representative Monte Carlo analysis of three dispersed cells selected at random from the data pooled from both Webb et al. and Liu et al. (2007) data under a null hypothesis of $1/f$-type noise (A-C) and a homogenous Poisson process (D-F). Note that the spectral properties of the Poisson process change according to the intensity of the process; this causes the 99^{th} quantile to have a different shape between plots. Note that under both noise models, both the circadian periods and the infradian periods when identified appear to be statistically significant at the $p < 0.01$ level; in particular, though shot noise is capable of generating the observation of spurious long periods, the majority of observed long period behavior remains statistically significant.

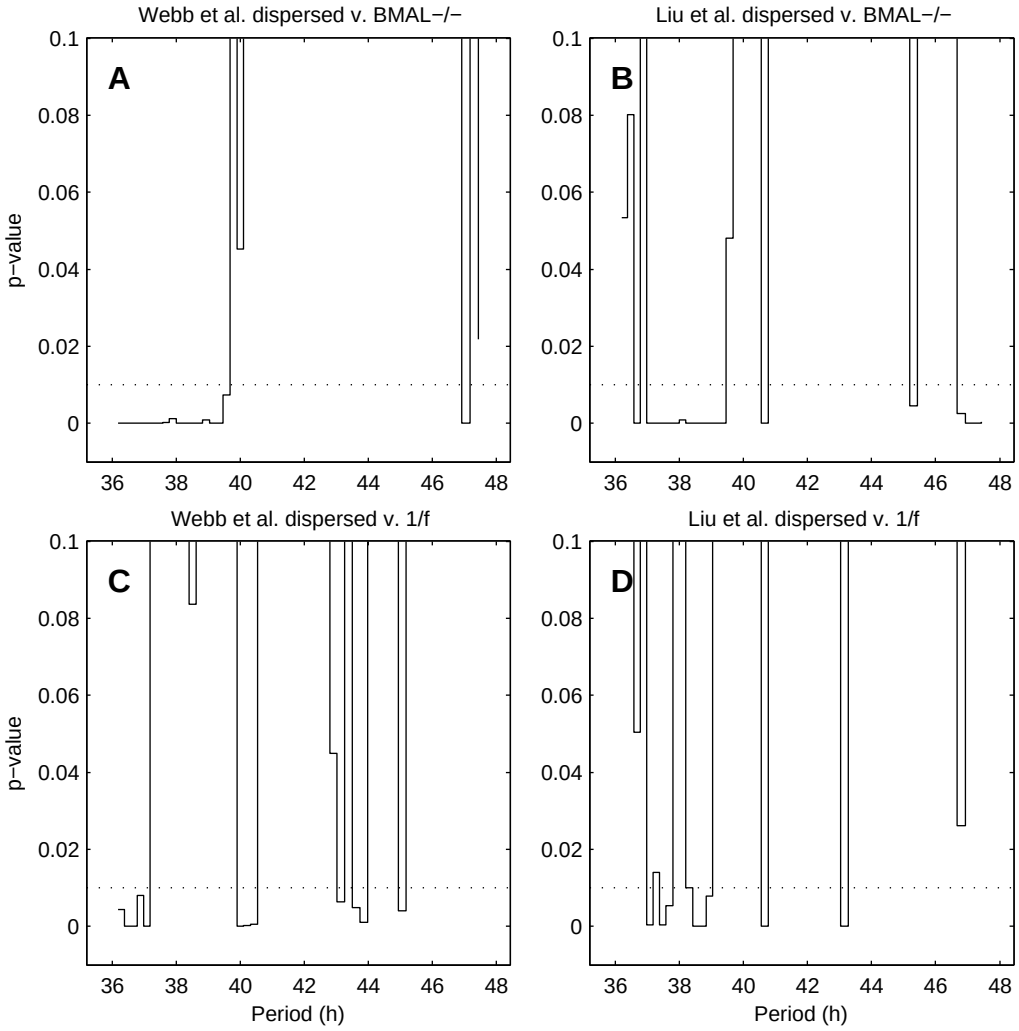

Figure S7: Plot of p-value versus period for infradian periods in dispersed cell data from both Webb et al. (A,C) and Liu et. al (B,D). The p-values are plotted against two different reference distributions as noted in the titles; $1/f$-type noise (A,C) and a distribution derived from the BMAL1 knockout data (B,D).

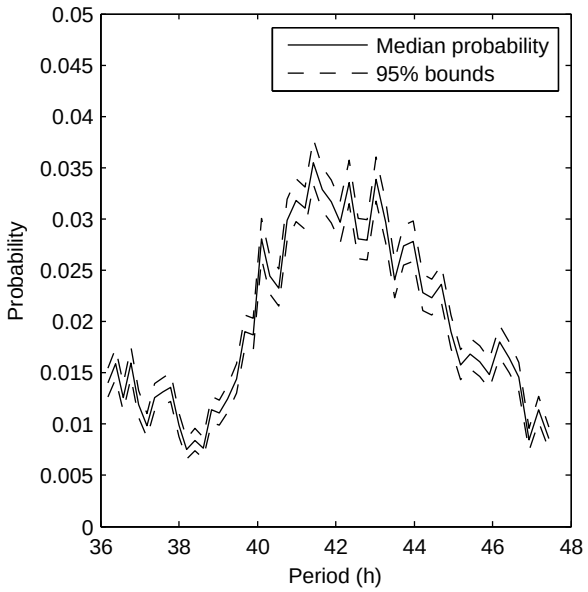

Figure S8: Distribution of infradian periods in BMAL1 knockout. Median and upper/lower 95% bounds are shown. Note that confidence bounds have been drawn on the sorted set neglecting to account for the sum-to-one constraint inherent in the Dirichlet distribution, and hence represent worst-case scenarios. The distribution displays a notably non-flat period distribution, favoring periods in roughly the 40 to 46 hour range.

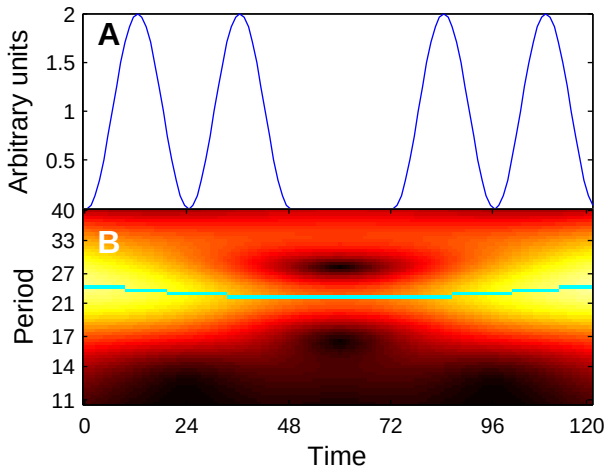

Figure S9: The effect of missed periods on the CWT ridge: a single skipped period produces only a slight distortion of the instantaneous period estimate for the oscillator. Units for the Y axis of panel A are arbitrary.

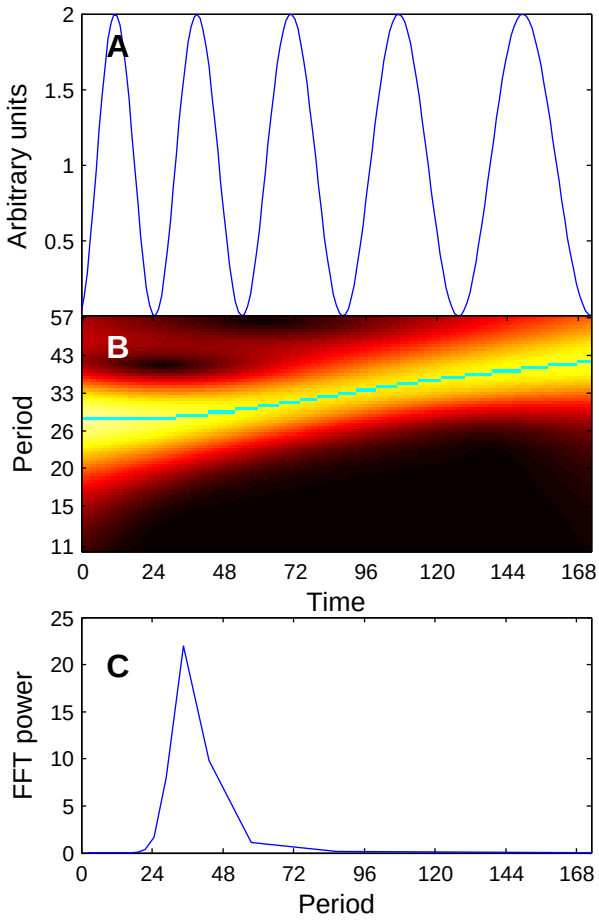

Figure S10: The effect of a signal with an increasing period (A) on the CWT ridge (B) and the FFT estimate (C). Note that the FFT incorrectly estimates a single fixed period for the signal, while the CWT ridge correctly estimates the linear change in period over time. As in Figure S9 the units for panel A are arbitrary.